

Supporting Information

1. Experimental Section

1.1 Preparation of air cathode

The catalyst inks of the initial full battery test were the mixtures of 5 mg commercial 20% Pt/C, 950 μ l isopropyl alcohol and 50 μ l 5wt% NafionTM solution. Press the stainless steel mesh onto the hydrophobic breathable film and then apply the 200 μ l ink to one side of the stainless steel mesh. The catalyst for cyclic charge-discharge test were the mixtures of 2.5 mg commercial 20% Pt/C and 2.5 mg RuO₂.

1.2 Characterizations

X-ray diffraction (XRD) analysis was performed using PANalytical (X'Pert3Powder) and PANalytical (Aeris) type X-ray diffractometers equipped with Cu K α radiation (40 kV, 44 mA) at a scanning speed of 5° min⁻¹. Zinc flakes indicate morphology and zinc dendrites were observed using a SU8220 (Hitachi) cold field emission scanning electron microscope (SEM) with an energy dispersion spectrometer (EDS). X-ray photoelectron spectroscopy (XPS) was acquired on an Escalab 250Xi (Thermo Fisher, UK) using a monochromatic Al K α source.

1.3 Electrochemical measurements

The Zn||Zn symmetric cells, Zn||Cu asymmetric cells and Zn||20% Pt/C full cells were used 0.5 mm-thick zinc plates, and alkaline electrolytes. All cell performances were evaluated on a battery testing equipment (LAND CT3001A 1U system, China).

Tafel plots, open-circuit potential test (OCPT) and EIS were measured in different electrolytes using a three-electrode system. The three-electrode system with Zn foil as the work electrode, Platinum electrode as the counter electrode and 3.5M Ag/AgCl as the reference electrode. Electrochemical impedance spectroscopy (EIS) was measured in a frequency range of 100 kHz to 0.1 Hz with AC amplitude of 5 mV. The above electrochemical tests were carried out on an electrochemical workstation (a CHI 760E electrochemical workstation, China).

Cyclic voltammetry (CV) test for the Zn||Zn symmetric cells as measured in a voltage range from -0.2 to 0.2 V at a scan rate of 1.0 mV s^{-1} . EIS for the Zn||Zn symmetric cells was used in the same testing conditions as the three electrode system.

Overpotential (η) test for Zn||Cu asymmetric cells were conducted at a constant current of 10 mA cm^{-2} for 2 hours. The cut-off voltage for charging of Coulombic Efficiency CE test was 0.6 V.

The assembled Zn||20% Pt/C (Zn||20% Pt/C + RuO_2) full cells were tested on a CHI 760E electrochemical workstation and a LAND CT3001A 1U system. The open-circuit voltage and the polarization curves for power density were collected on the former, and the other tests were recorded on the latter. The power density curve was obtained from LSV testing, the LSV test started at 1.6 V and ended at 0.2 V at a scanning speed of 0.5 mV s^{-1} . The galvanostatic charge-discharge (GCD) was run under 5 mA cm^{-2} for 10 min per charge/discharge step until the batteries were out of action or cycled 3000 times. the batteries were out of action or cycled 3000 times.

1.4 Computation methods

The density functional theory (DFT) calculations were carried out with the VASP code^[1]. The Perdew-Burke-Ernzerhof (PBE) functional within generalized gradient approximation (GGA)^[2] was used to process the exchange–correlation, while the projectoraugmented-wave pseudopotential (PAW)^[3] was applied with a kinetic energy cut-off of 500 eV , which was utilized to describe the expansion of the electronic eigenfunctions. The vacuum thickness was set to be 50 Å to minimize interlayer interactions. The Brillouin-zone integration was sampled by a Γ -centered $4 \times 4 \times 1$ Monkhorst–Pack k-point. All atomic positions were fully relaxed until energy and force reached a tolerance of $1 \times 10^{-6} \text{ eV}$ and 0.01 eV/Å , respectively. The dispersion corrected DFT-D method was employed to consider the long-range interactions^[4]. The adsorption energies of molecule on Zn surfaces can be calculated using the following equation:

$$E_{\text{ads}} = E_{\text{iso}} + \text{slab} - (E_{\text{iso}} + E_{\text{slab}})$$

Where:

the $E_{\text{iso}} + \text{slab}$, E_{iso} and E_{slab} are the energies of slab covered with adsorbates, the isolated

adsorbate molecule, and the clean slab, respectively.

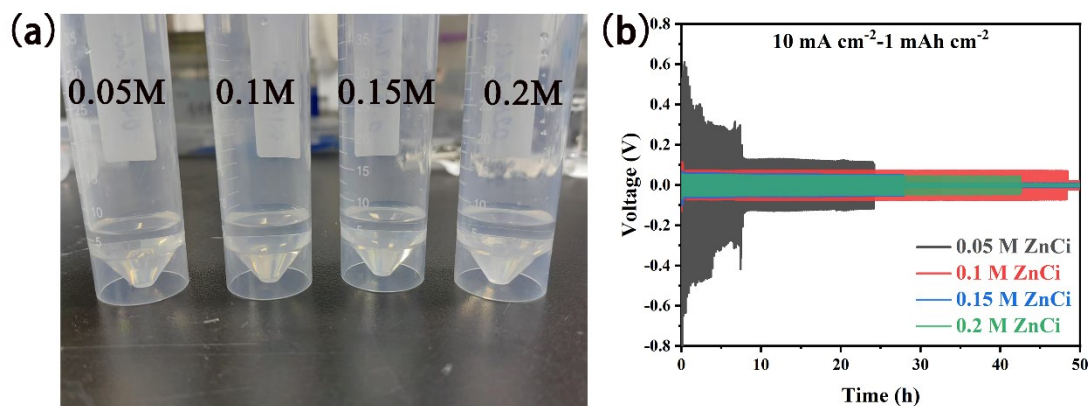


Fig S1 (a) Optical photos of different concentrations of ZnCi electrolyte; (b) Symmetrical cell testing of ZnCi electrolytes with different concentrations.

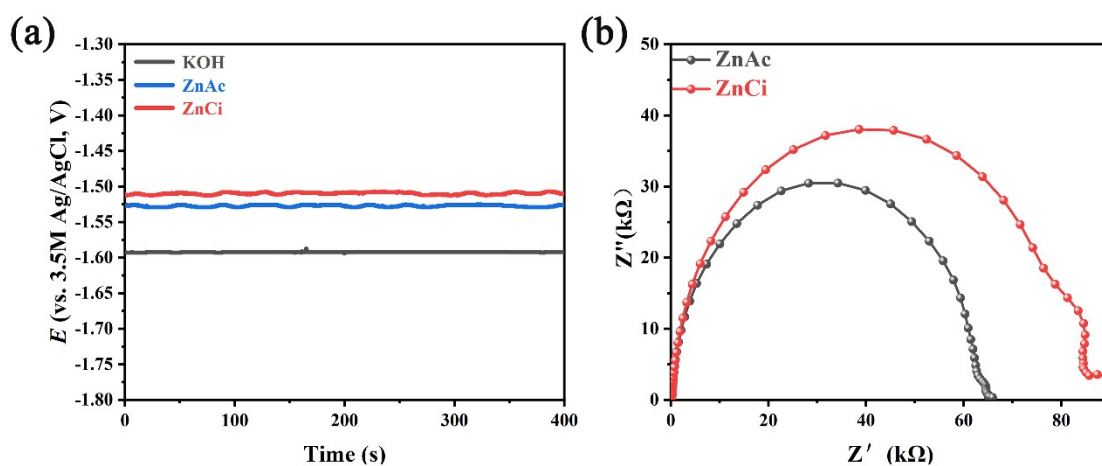


Fig S2 Open-circuit potential test (OCPT) of different electrolytes in three-electrode system (a) ; EIS of different electrolytes in three-electrode system (b).

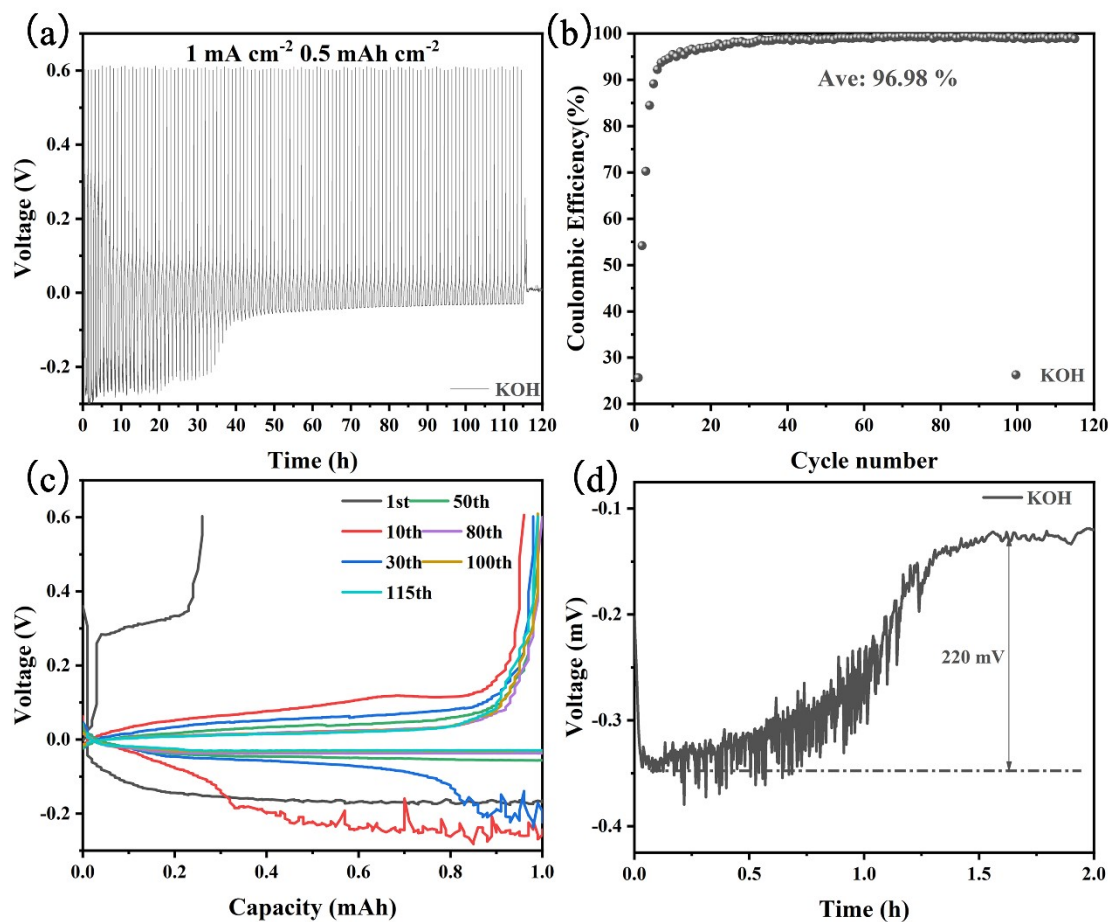


Fig. S3 Cycling performance of Zn||Cu asymmetric cells with pure KOH as electrolyte (a); Coulombic Efficiency CE of the Zn||Cu asymmetric cells (b); Voltage-capacity curves for the selected cycles in the CE test using the 6 M KOH electrolyte (c); (d) overpotential (η) test

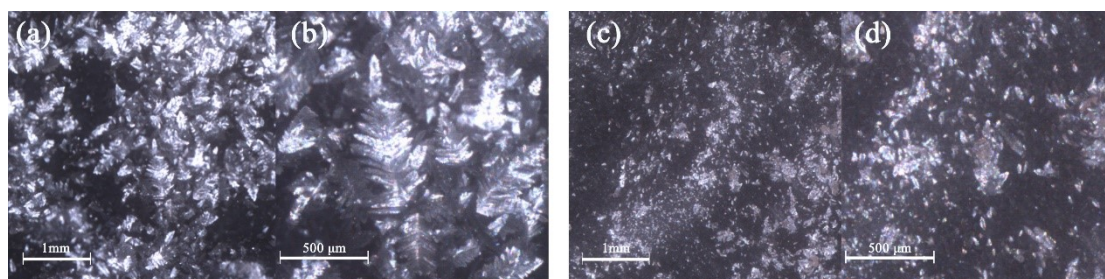


Fig S4 Light microscopy images of deposited Zn anode in ZnCi electrolyte (a, b) and ZnAc electrolyte (c, d).

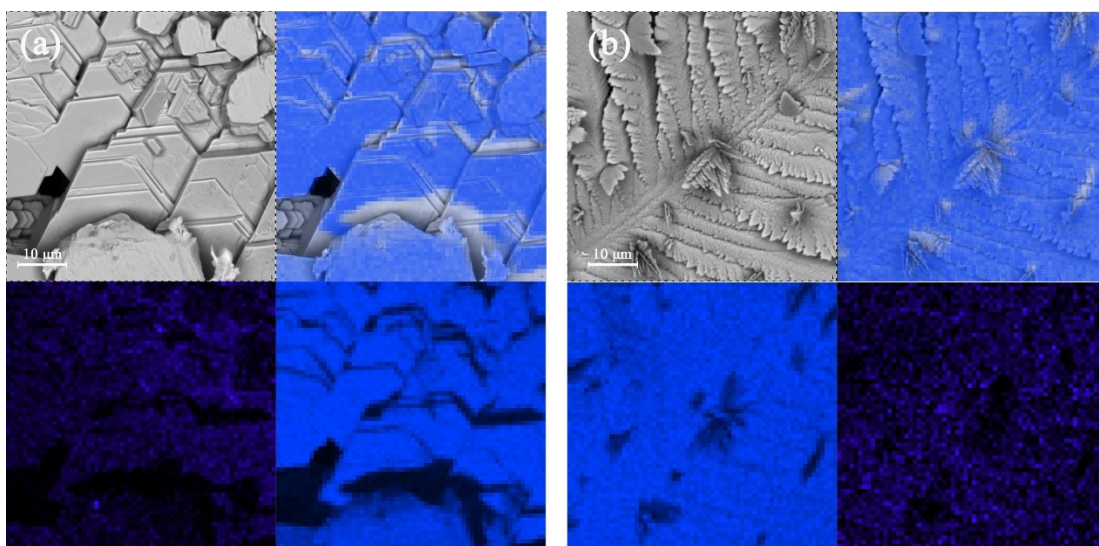


Fig S5 EDS mapping images of ZnCi electrolyte (a) and ZnAc electrolyte (b)

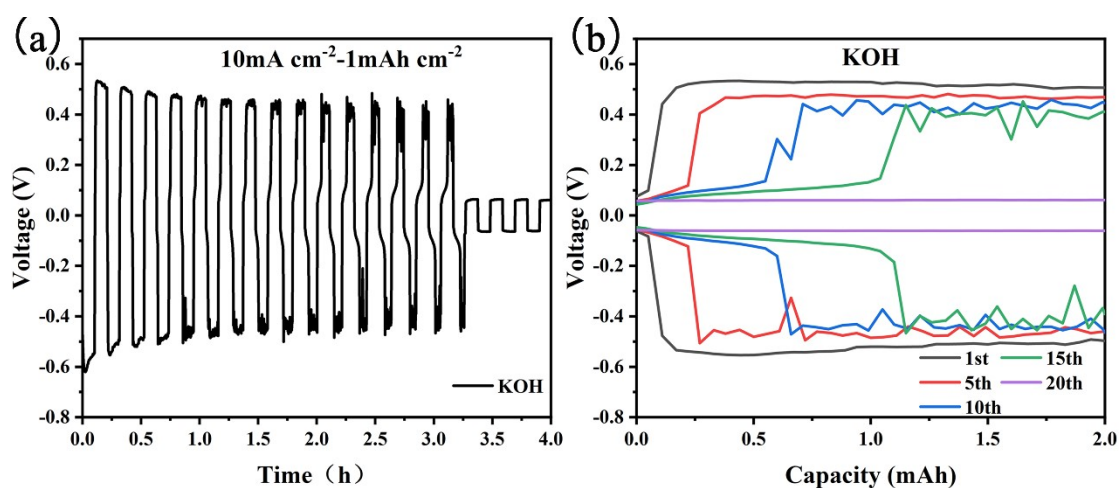


Fig. S6 Cycling performance of Zn||Zn symmetric cells in 6 M KOH at 10 mA cm⁻² (a) ; (b) voltage-capacity curves at a current density of 10 mA cm⁻² for the selected cycles the cell-KOH

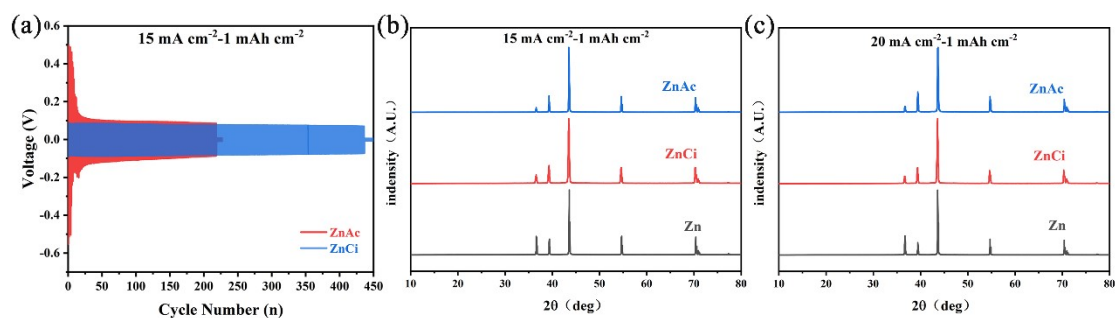


Fig. S7 Cycling performance of Zn||Zn symmetric cells in different electrolytes at 15 mA cm⁻² (a); XRD patterns of Zn anode in different electrolytes at 15 mA cm⁻² (b) and 20 mA cm⁻² (c).

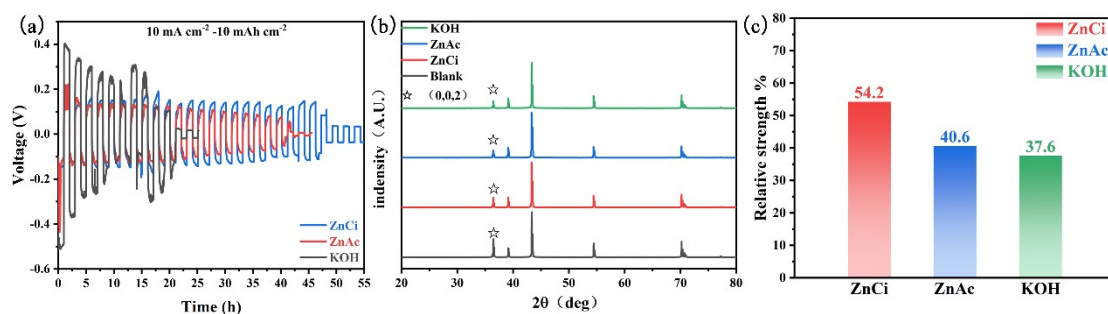


Fig. S8 Cycling performance of Zn||Zn symmetric cells in different electrolytes at 10 mA cm⁻² 10 mAh cm⁻² (a); (b) XRD patterns of Zn anode in different electrolytes after the experimental of (a) ; (c) The retention rate of (002) crystal plane in different electrolytes after the cycle.

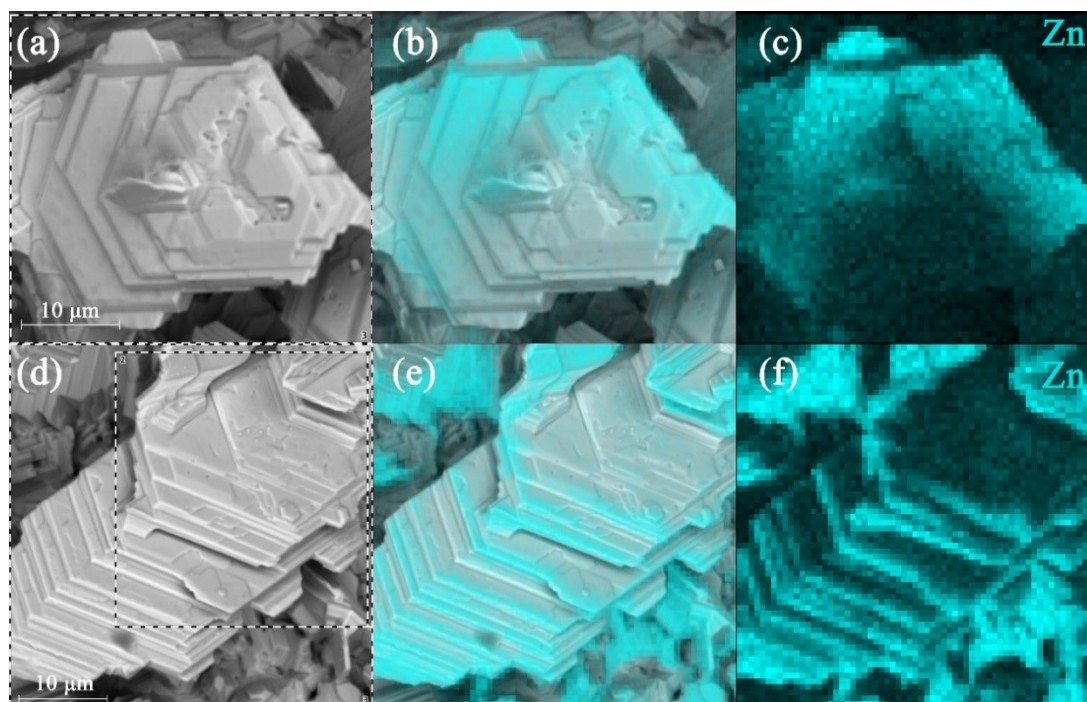


Fig. S9 EDS mapping images of ZnCl electrolyte (a-c) and ZnAc electrolyte (d-f) after Zn||Zn symmetrical cells test

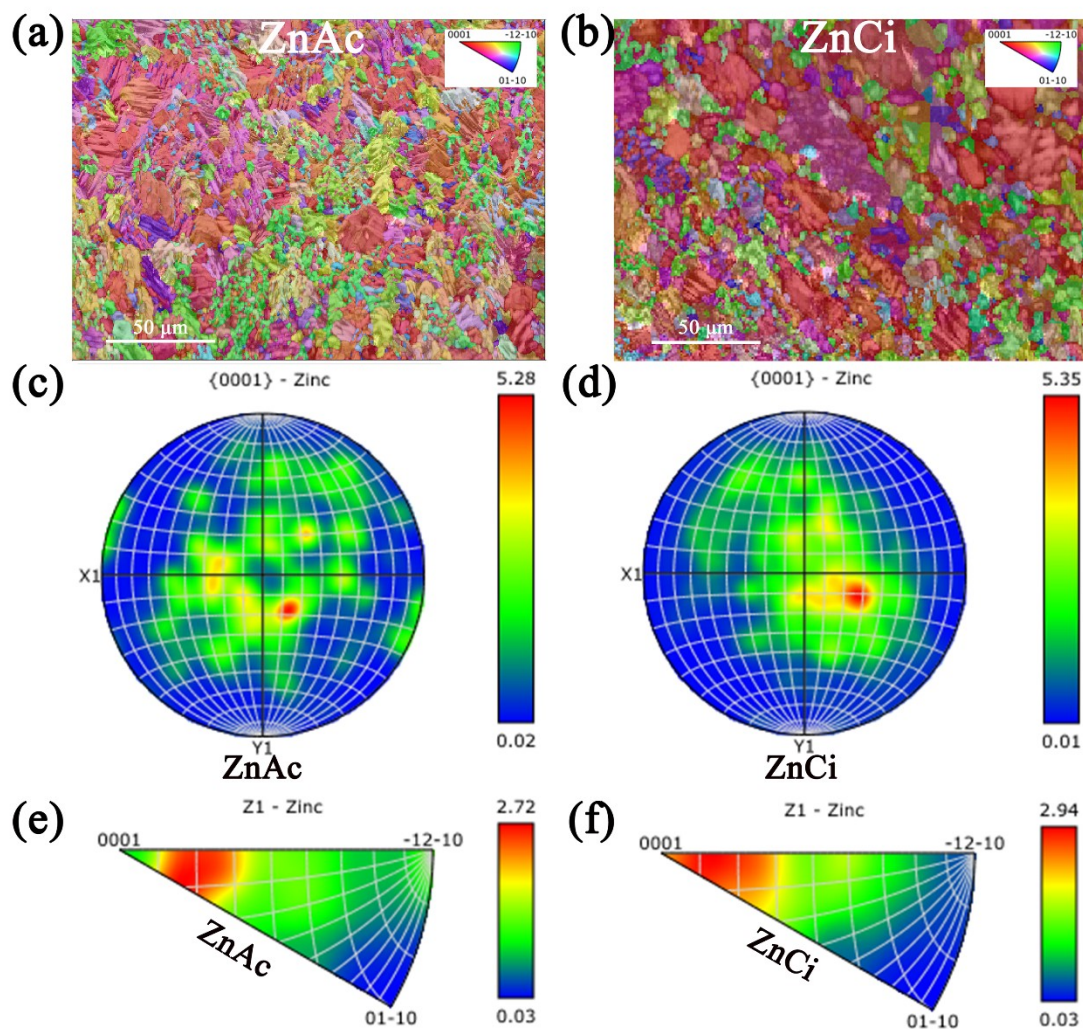


Fig. S10 EBSD images of Zn after cycling in (a) ZnAc and (b) ZnCi, respectively, inset is the inverse pole Figures (IPF) triangle map, in which the red color represents the (002) crystallographic direction. (c–d) Corresponding polar diagrams of the EBSD image. The inverse pole figure of (e) ZnAc electrolyte and (f) ZnCi electrolyte.

Table S1. Tafel parameters for different electrolytes

electrolyte	Equilibrium potential	Corrosion current	Cathode Tafel slope	Anode Tafel slope	inhibition efficiency
KOH	-1.595 V	0.389 μ A	-5.968 V dec ⁻¹	5.905 V dec ⁻¹	/
ZnAc	-1.528 V	0.377 μ A	-6.103 V dec ⁻¹	5.910 V dec ⁻¹	3.08%
ZnCi	-1.512 V	0.304 μ A	-6.180 V dec ⁻¹	5.553 V dec ⁻¹	21.85 %

Reference

- [1] Steneteg P, Abrikosov I A, Weber V, et al. Wave function extended Lagrangian Born-Oppenheimer molecular dynamics. Physical Review B, 2010, 82(7): 202109108.
- [2] Perdew, Burke, Ernzerhof. Generalized Gradient Approximation Made Simple. Physical Review Letters, 1996, 77(18): 202109108.
- [3] Blochl. Projector augmented-wave method. Physical review. B, Condensed matter, 1994, 50(24): 202109108.
- [4] Grimme S. Semiempirical GGA-type density functional constructed with a long-range dispersion correction. Journal of Computational Chemistry, 2006, 27(15): 202109108.